

Serendipity and the SDSS: Discovery of the Largest Known Planetary Nebula on the Sky

Paul C. Hewett,¹

phewett@ast.cam.ac.uk

Michael J. Irwin,¹

mike@ast.cam.ac.uk

Evan D. Skillman,^{1,2}

skillman@astro.umn.edu

Craig B. Foltz,³

cfoltz@nsf.gov

Jon P. Willis,^{4,5}

jwillis@uvic.ca

Stephen J. Warren⁶

s.j.warren@imperial.ac.uk

and Nicholas A. Walton¹

naw@ast.cam.ac.uk

ABSTRACT

¹Institute of Astronomy, Madingley Road, Cambridge, CB3 0HA, UK

²Department of Astronomy, University of Minnesota, 116 Church Street, SE, Minneapolis, MN 55455

³Division of Astronomical Sciences, National Science Foundation, Room 1045, 4201 Wilson Blvd, Arlington, VA 22230

⁴European Southern Observatory, Alonso de Cordoba 3107, Vitacura, Casilla 19001, Santiago 19, Chile

⁵Current address: Department of Physics & Astronomy, University of Victoria, PO Box 3055 STN CSC, Victoria, BC, V8W 3P6 Canada

⁶Astrophysics Group, Blackett Laboratory, Imperial College London, Prince Consort Road, London SW7 2BW, UK

Investigation of spectra from the Sloan Digital Sky Survey reveals the presence of a region of ionized gas of $> 2^\circ$ diameter centered approximately at $\alpha = 10^h 37^m$ $\delta = -00^\circ 18'$ (J2000) (Galactic coordinates $l = 248, b = +48$). [O III] 4959,5007 emission is particularly strong and emission from H α and [N II] 6548,6583 is also detectable over a substantial area on the sky. The combination of emission line ratios, the close to zero heliocentric radial velocity and the morphology of the structure are consistent with an identification as a very nearby planetary nebula. The proximity of the hot, DO white dwarf PG 1034+001 further strengthens this interpretation. The object is: i) the largest planetary nebula on the sky, ii) certainly closer than any planetary nebula other than Sh 2–216, iii) the first to be unambiguously associated with a DO white dwarf. A parallax distance for PG 1034+001 would establish whether the structure is in fact the closest, and one of the physically largest, planetary nebula known.

Subject headings: ISM: planetary nebulae: individual: (Hewett 1)—Stars: white dwarfs: individual (PG1034+001)

1. Introduction

The availability (Abazajian et al. 2003) of a significant fraction of the spectra and images from the Sloan Digital Sky Survey (SDSS) (York et al. 2000) provides a unique resource for the investigation of a wide variety of astrophysical phenomena. The quality and scale of the database are such that a number of serendipitous discoveries can be expected in the coming years. In this *Letter* we report the discovery, using SDSS spectra of unrelated objects, of the largest known planetary nebula (PN) on the sky.

2. Data

In the course of a search for SDSS spectra that show the signature of two objects, at different redshifts, the distinctive presence of the [O III] 4959,5007 doublet, at essentially rest-frame wavelength, in several adjacent spectra was noted. A more targeted search employed a simple 41-pixel (57 Å) median filter to generate a “continuum” which was then subtracted from the original spectrum to produce a “difference” spectrum. Emission lines were identified in individual and composite difference-spectra using standard matched-filter techniques. The search revealed the presence of [O III] 4959,5007 in more than 100 spectra with the flux in the [O III] 5007 line ranging from $1.6 \times 10^{-15} \text{erg s}^{-1} \text{cm}^{-2}$ down to the limit of

detectability of $\simeq 8 \times 10^{-17} \text{erg s}^{-1} \text{cm}^{-2}$. Surface brightnesses, per square arcsecond, can be obtained from the fluxes measured in the spectra by dividing by the fibre area (7.1 arcsec^2).

The detections were confined to objects in a region several degrees across centered at approximately $\alpha = 10^{\text{h}}37^{\text{m}}$ $\delta = -00^{\circ}18'$ or $159.3^{\circ}, -0.3^{\circ}$ (J2000). $\text{H}\alpha$, $\text{H}\beta$, [N II] 6548,6583 and [S II] 6718,6732 emission lines were also present in spectra in the same region. Figure 1 shows the spatial distribution of the spectra with detectable [O III] 4959,5007 (\bullet), $\text{H}\alpha$ (\circ), and [N II] 6583 (\times). The hatched area, extending to a radius of 1° from $10^{\text{h}}37^{\text{m}} -00^{\circ}18'$, indicates a region where composite spectra, derived using groups of 25 spectra without individual [O III] 4959,5007 detections, show unambiguous evidence of [O III] 4959,5007 emission. Positions of objects with SDSS spectra for which no individual detections were obtained are also indicated (\cdot).

Figure 2 shows the wavelength regions containing [O III] 4959,5007 and $\text{H}\alpha$, [N II] 6548,6583 plus [S II] 6718,6732 for a composite, continuum-subtracted, spectrum made using all the galaxy and quasar spectra within 0.5° of $10^{\text{h}}37^{\text{m}} -00^{\circ}18'$ (upper panels). Another composite, using objects from a more distant arc-shaped region to the south-west is also shown (lower panels). The arc-shaped region is defined by radial distance $0.7^{\circ} - 1.3^{\circ}$ from $10^{\text{h}}37^{\text{m}} -00^{\circ}18'$ and angular extent $180^{\circ} \leq \text{PA} \leq 315^{\circ}$ relative to the same position. The composite from the central region displays very strong [O III] 4959,5007 and, while $\text{H}\alpha$ and [N II] 6548,6583 are clearly visible, shows the relative weakness of the hydrogen lines. The composite spectrum from large radii to the south-west illustrates the fall-off in the strength of the [O III] 4959,5007 emission with radius and the marked variation in the $\text{H}\alpha$ /[N II] 6548,6583 ratio with position. The spectra of stars were not included in the generation of the composite spectra. To avoid contamination of the composite spectrum from unrelated emission and absorption features, wavelength regions associated with strong emission and absorption features in the rest-frames of the galaxy and quasar spectra were excluded from the construction of the composite spectra.

Examination of the sky-subtracted sky spectra in SDSS plates 273 and 274, which contain the region, show no evidence for absorption at the location of any of the emission lines. The lack of absorption confirms that the emission line fluxes associated with the $\simeq 2^{\circ}$ region, centered on $10^{\text{h}}37^{\text{m}} -00^{\circ}18'$, are not affected significantly by more extended emission on scales of $\sim 5^{\circ}$.

The resolution of the SDSS spectra ($\simeq 3.1\text{\AA}$) precludes a reliable determination of the radial velocity. The centroids of the [O III] 4959,5007, $\text{H}\alpha$ and [N II] 6583 emission lines in a composite of the 38 spectra showing the strongest [O III] 4959,5007 emission give a heliocentric radial velocity of $-5 \pm 5 \text{ km s}^{-1}$. However, the amplitude is comparable to the wavelength accuracy of the SDSS spectra and variations of several tens of km s^{-1} are evident

Table 1: Emission Line Fluxes in the $< 0.5^\circ$ Composite Spectrum

Species	Wavelength (Ångstroms)	Flux ($10^{-17} \text{erg s}^{-1} \text{cm}^{-2}$)
[Ne III]	3870	6.5 ± 1.0
H β	4861	1.0 ± 0.8
[O III]	4959	10.6 ± 1.5
[O III]	5007	38.6 ± 3.0
[N II]	6548	1.8 ± 0.5
H α	6563	7.7 ± 1.2
[N II]	6583	5.1 ± 1.0
[S II]	6717	1.7 ± 0.7

from spectrum to spectrum. In summary, the heliocentric velocity of the gas is consistent with a value of $0 \pm 20 \text{ km s}^{-1}$.

The large angular extent and small radial velocity suggest a relatively local origin for the ionized gas. The Galactic coordinates, $l = 248, b = +48$, further suggest that the gas is within a few hundred parsecs if the object lies within the Galactic disc. The weakness of the hydrogen lines and the lack of any bright early-type stars in the vicinity of the nebula rule out identification as an H II region.

3. Further Investigations

Narrow-band imaging of the [O III] 4959,5007 lines ($\lambda_c = 5008\text{Å}$, $\Delta\lambda = 100\text{Å}$) and the H α + [N II] 6548,6583 lines ($\lambda_c = 6568\text{Å}$, $\Delta\lambda = 95\text{Å}$) was undertaken using the Wide Field Camera (WFC) on the Isaac Newton Telescope (INT) on the nights of 2003 May 1 and 21–27. Exposure times of 900 – 1200 s (H α) and 3×900 s [O III] were used, with shorter exposures of 600s for companion broad-band images in g and r passbands. An area of roughly a square degree was imaged in both [O III] and H α . After processing through the INT WFC pipeline (Irwin & Lewis 2001) there was a clear detection of complex [O III] and H α nebulosity extending over the whole region, confirming the reality of the spectroscopic detections. The resulting continuum-subtracted, stacked [O III] and H α images are shown in Figure 3. The area visible in the images is indicated by the dashed outline in Figure 1. The centrally concentrated distribution of [O III] 4959,5007 emission is particularly striking. A distinctive feature present in the [O III] image is the arc-like structure visible at center-right.

In the $< 0.5^\circ$ composite (Figure 2a,b) the [O III] $\lambda 5007/\lambda 4959$ ratio of 3.6 ± 0.4 and the [N II] $\lambda 6583/\lambda 6548$ ratio of 2.8 ± 0.3 are both consistent with their theoretical values, which depend only on atomic physics for the conditions pertaining in PN, suggesting the spectrum provides useful diagnostic information (although new spectra of the high surface brightness features are needed). $H\beta$, which is clearly present in individual spectra with the strongest emission line fluxes, is barely detectable in the $< 0.5^\circ$ composite spectrum. The $H\alpha/H\beta$ ratio of 7.5 ± 3.5 indicates some reddening (formally $A_V = 0.9^{+0.3}_{-0.6}$). Relatively weak underlying absorption in the Balmer lines would help explain the low $H\beta$ flux while making little difference to the strength of $H\alpha$. The nearly reddening independent ratios of [N II] $\lambda 6583/H\alpha = 0.8 \pm 0.2$ and [N II] $\lambda 6583/[S II] \lambda 6716 = 2.9 \pm 1$ are both within the ranges observed in nitrogen-rich PN. The [O III] $\lambda 5007/H\beta$ ratio of 38 ± 10 is very high, although not unprecedented in PNs (and is biased high by the selection process). Further support for the classification as a PN comes from the detection of [Ne III] 3869. The absence of detectable emission from lines of He I and He II is consistent with normal abundances and the S/N of the composite spectrum. In summary, the emission line properties of both composite and individual spectra are consistent with the properties of a PN with a relatively hot central star.

Indeed, the images in the atlas of ancient PNs (Tweedy & Kwitter 1996) contain some strikingly similar structures. The centrally concentrated morphology evident in the distribution of [O III] 4959,5007 emission is common and large variations in emission line ratio, including strong [N II] and [S II] towards the outer edges of old PNs, due to interactions between the ejecta and the ambient interstellar medium, are often seen. The most unusual property of the structure reported here is the angular size, which, at $> 2^\circ$ diameter exceeds that of Sh 2–216, also long considered the closest PN, with an angular size of 1.6° (Fesen, Blair, & Gull 1981; Tweedy & Napiwotzki 1992).

Since there was no plausible ionizing source in the SDSS photometric catalogue, the APM sky survey catalogues were used for further investigation of potential ionizing sources of radiation. In a 1.5° region centered on $10^h 37^m -00^\circ 20'$ one bright candidate ionizing source stood out at $10^h 37^m 03.875^s -00^\circ 08' 19.59''$ J2000 (Epoch 1982), with UKST plate magnitudes and colors of $R = 13.06$ and $B_J - R = -0.47$ (see Figure 4). Using the UKST plate as a reference frame the refined APM POSS1 (Epoch 1952) position of this source is $10^h 37^m 04.047^s -00^\circ 08' 20.53''$ J2000, giving a high proper motion of $-86 \pm 5, +31 \pm 5$ mas yr $^{-1}$. The color, magnitude and proper motion suggested the object was probably a hot WD at around ≈ 100 pc and a search, utilizing Simbad, reveals the source is PG 1034+001, a bright, $V = 13.23$ (Landolt 1992), DO white dwarf. A very crude kinematic age of $\sim 130,000$ yr, can be derived from the radius of the PN, $\simeq 1^\circ$ at a distance of $\simeq 150$ pc, and a typical expansion velocity of PN, $\simeq 20$ km s $^{-1}$. The WD is currently close to the center of the region over which

detectable emission is present in the SDSS spectra. The WD is also in close proximity, $\approx 15'$, to the region showing the strongest [O III] 4959,5007 emission, however, the proper motion vector for the WD indicates a position for the WD to the east of the present location at the time the PN was formed. If the arc-like feature visible in Figure 3 represents a shock, or a boundary, associated with material ejected at the time the PN was formed then a lower limit to the kinematic age for the PN can be estimated by extrapolating the motion of the white dwarf back to the origin of the radius of curvature of the arc. The resulting limit on the age, $> 50,000 \pm 10,000$ yr is plausible but an understanding of the nature of the arc-like feature is necessary to validate the argument. An age of $\approx 100,000$ yr is consistent with all the evidence but measurement of the expansion velocity and a more complete mapping of the morphology of the emission will provide a much improved estimate.

4. Discussion

Given that all observations are consistent with a PN nature for the newly discovered nebulosity, we designate it Hewett 1. The proximity of the DO white dwarf PG 1034+001 (Wesemael, Green, & Liebert 1985) makes it probable that PG 1034+001 is responsible for the ionizing radiation. Werner, Dreizler, & Wolff (1995) derived a spectroscopic distance for PG 1034+001 of 155^{+58}_{-43} pc and confirmation of the association would make Hewett 1 one of the closest PNs known (Napiwotzki 2001), the 2° diameter corresponding to a physical size of 3.5–7.0 pc for the likely distance range of 100–200 pc. Again, Sh 2–216 provides the current benchmark, with a trigonometric distance of 130^{+9}_{-8} pc (Harris et al. 1997) and a physical size of $\simeq 3.5$ pc. A parallax determination for PG 1034+001 would establish whether Hewett 1 is even closer.

Notwithstanding targeted searches (Werner et al. 1997), very few PNs are known to be associated with non-DA (hydrogen poor) white dwarfs. Hewett 1 may be the first PN to be discovered associated with a DO white dwarf, although PG 0108+101 (Reynolds et al. 1987) and PG 0109+111 (Werner et al. 1997) have candidate nebulae, neither detection is regarded as secure. Since DO white dwarfs are thought to evolve from PG 1159 stars (see Dreizler & Werner 1996, and references therein), it will be of interest to compare the properties of Hewett 1 both to the PNs associated with PG 1159 stars (Napiwotzki 1999) and theoretical models (Górny & Tylenda 2000). The derivation of a reliable age for the PN associated with PG 1034+001 will be of particular interest for constraining the time scales associated with the late-stages of evolution of post-asymptotic giant branch stars and the origin of PG 1159 stars and helium-rich WDs.

EDS is grateful for the hospitality of the IoA during his sabbatical visit and we thank Alan McConnachie for assisting with the INT imaging observations. We are grateful to the anonymous referee who provided a detailed review of the original manuscript. This paper includes observations made with the Isaac Newton Telescope, operated on the island of La Palma by the Isaac Newton Group in the Spanish Observatorio del Roque de los Muchachos of the Instituto de Astrofísica de Canarias. Funding for the Sloan Digital Sky Survey (SDSS) has been provided by the Alfred P. Sloan Foundation, the Participating Institutions, the National Aeronautics and Space Administration, the National Science Foundation, the U.S. Department of Energy, the Japanese Monbukagakusho, and the Max Planck Society. The SDSS Web site is <http://www.sdss.org/>.

REFERENCES

- Abazajian, K. et al. 2003, AJ, in press (astro-ph/0305492)
- Dreizler, S. & Werner, K. 1996, A&A, 314, 217
- Fesen, R. A., Blair, W. P., & Gull, T. R. 1981, ApJ, 245, 131
- Górny, S. K. & Tylanda, R. 2000, A&A, 362, 1008
- Harris, H. C., Dahn, C. C., Monet, D. G., & Pier, J. R. 1997, IAU Symp. 180: Planetary Nebulae, 180, 40
- Irwin, M. & Lewis, J. 2001, New Astronomy Review, 45, 105
- Landolt, A. U. 1992, AJ, 104, 340
- Napiwotzki, R. 1999, A&A, 350, 101
- Napiwotzki, R. 2001, A&A, 367, 973
- Reynolds, R. J. 1987, ApJ, 315, 234
- Tweedy, R. W. & Kwitter, K. B. 1996, ApJS, 107, 255
- Tweedy, R. W. & Napiwotzki, R. 1992, MNRAS, 259, 315
- Werner, K., Bagschik, K., Rauch, T., & Napiwotzki, R. 1997, A&A, 327, 721
- Werner, K., Dreizler, S., & Wolff, B. 1995, A&A, 298, 567
- Wesemael, F., Green, R. F., & Liebert, J. 1985, ApJS, 58, 379

York, D. G. et al. 2000, *AJ*, 120, 1579

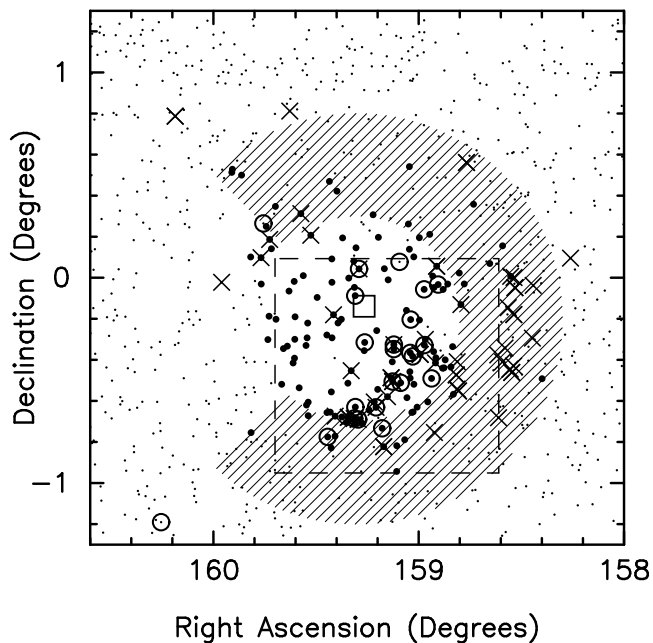


Fig. 1.— Spatial distribution of spectra with detectable [O III] 4959,5007 (●), $H\alpha$ (○), and [N II] 6583 (×). The hatched area indicates a region where composite spectra also show unambiguous evidence of [O III] 4959,5007 emission. Positions of objects with SDSS spectra for which no individual detections were obtained are also indicated (·). The dashed outline shows the area included in the narrow-band images of Figure 3. The location of the white dwarf PG 1034+001 is marked by a □.

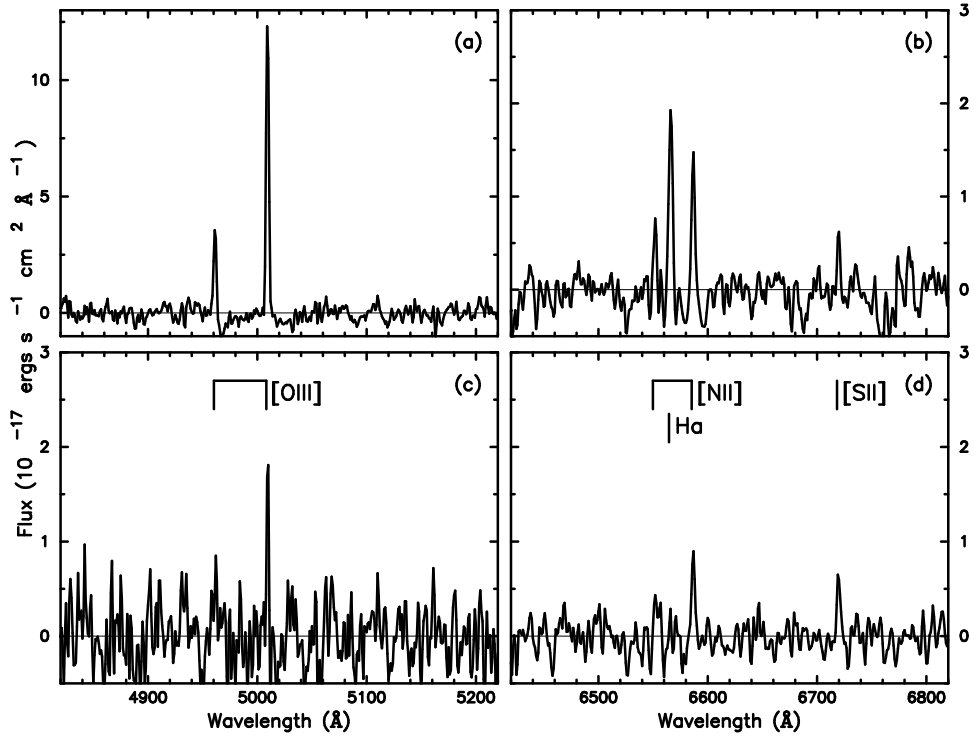


Fig. 2.— Wavelength regions containing [O III] 4959,5007 and H α , [N II] 6548,6583 plus [S II] 6718,6732 for a composite, continuum-subtracted, spectrum made using all the galaxy and quasar spectra within 0.5° of $10^h37^m - 00^\circ18'$ (upper panels). Another composite, using objects with position angles $180^\circ \leq PA \leq 315^\circ$ lying between $0.7^\circ - 1.3^\circ$ from $10^h37^m - 00^\circ18'$ is also shown (lower panels). The composite from the central region displays very strong [O III] 4959,5007 and, while H α and [N II] 6548,6583 are clearly visible, shows the relative weakness of the hydrogen lines. The composite spectrum from large radii to the south-west illustrates the fall-off in the strength of the [O III] 4959,5007 emission with radius and the marked variation in the H α /[N II] 6548,6583 ratio with position.

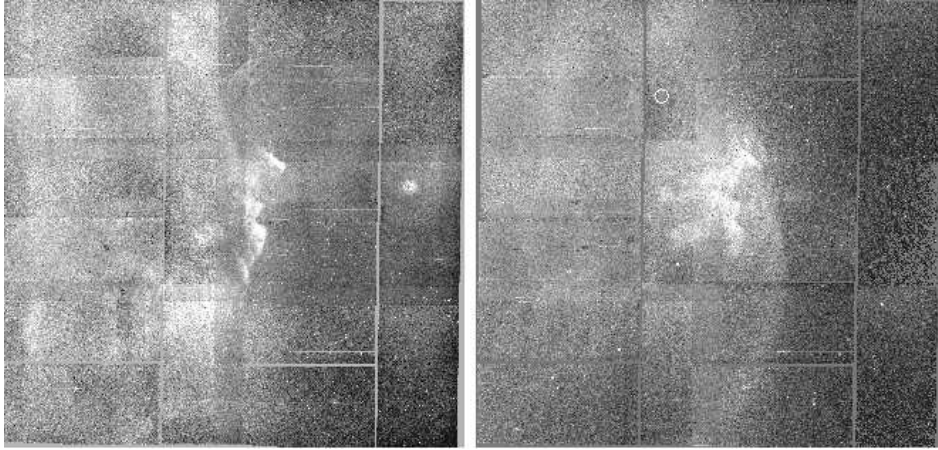


Fig. 3.— The left hand panel shows a mosaic of 6 continuum-subtracted pointings in $H\alpha$ + [N II] while the right panel shows the equivalent for [O III]. The images are approximately 0.8° on a side with North to the top and East to the left. The position of the white dwarf PG 1034+001 is indicated by a circle in the [O III] image. Emission with complex structure is evident in the central regions of the images in both passbands. A well-defined arc, or boundary, is visible at center-right in the [O III] image.

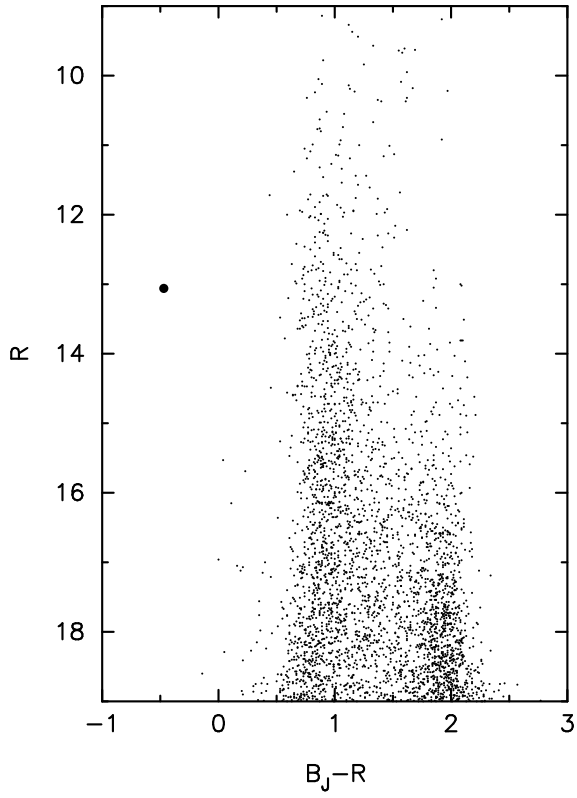


Fig. 4.— $B_J - R$ versus R color-magnitude diagram for objects within 0.75° of $10^h37^m -00^\circ18'$ using the APM sky catalogue magnitudes of UK Schmidt Telescope B_J and R plates. All objects classified as stellar are plotted (\cdot) with the location of the white-dwarf PG 1034+001 highlighted (\bullet).